IEEE Access
Multidisciplinary | Rapid Review | Open Access Journal

Received June 29, 2018, accepted August 5, 2018, date of publication August 10, 2018, date of current version September 5, 2018.

Digital Object Identifier 10.1109/ACCESS.2018.2864892

IQI Mitigation for Narrowband IoT Systems With OFDM-IM

ARMED TUSHA[1], SEDA DOĞAN[1], AND HÜSEYİN ARSLAN[1,2], (Fellow, IEEE)
[1]Department of Electrical and Electronics Engineering, Istanbul Medipol University, 34810 Istanbul, Turkey
[2]Department of Electrical Engineering, University of South Florida, Tampa, FL 33620, USA

Corresponding author: Armed Tusha (atusha@st.medipol.edu.tr)

ABSTRACT The crucial aim for 5G narrowband Internet of Things (NB-IoT) is to support massive connectivity with wide coverage area, low power consumption, low hardware complexity, and low data rate. Direct conversion receiver (DCR) has a simple structure to fulfill NB-IoT requirements. However, a significant degradation has been observed on the performance of orthogonal frequency division multiplexing (OFDM) systems with the DCR due to in-phase and quadrature imbalance (IQI) at RF front-end. Estimation and mitigation of IQI in OFDM systems require an iterative receiver at the expense of high complexity and power consumption. In this paper, OFDM with index modulation (OFDM-IM) is proposed as a promising candidate in order to meet the demands of NB-IoT use cases. OFDM-IM-based systems carry data information not only by modulated subcarriers but also by indices of fractionally used subcarriers. A non-iterative and efficient receiver that exploits inactive subcarriers is introduced to mitigate the effect of IQI for NB-IoT with OFDM-IM. Cyclic redundancy check algorithm is used to investigate the accuracy of the receiver under IQI. Theoretical analysis and computer-based simulations show that the proposed non-iterative receiver for OFDM-IM in NB-IoT under IQI works very well in various scenarios. Moreover, our findings show that the OFDM-IM under IQI provides higher signal-to-interference ratio in comparison with classical OFDM.

INDEX TERMS IQI, NB-IoT, non-iterative estimation and mitigation, OFDM with index modulation (OFDM-IM).

I. INTRODUCTION

Narrowband Internet of Things (NB-IoT) provides Low Power Wide Area (LPWA) coverage via massive devices for next-generation use cases and applications [1]–[3]. In order to make massive connections possible over devices, NB-IoT should meet key performance requirements of IoT. The key requirements consist of user equipment (UE) with low complexity, low power consumption, long battery life and deployment flexibility [2]–[4]. For instance, smart metering and smart agriculture reduce cost and improve service quality by remotely accessing the devices, while smart parking reduces traffic and car accidents by connected vehicles. Some use cases for NB-IoT technology are illustrated in Fig. 1.

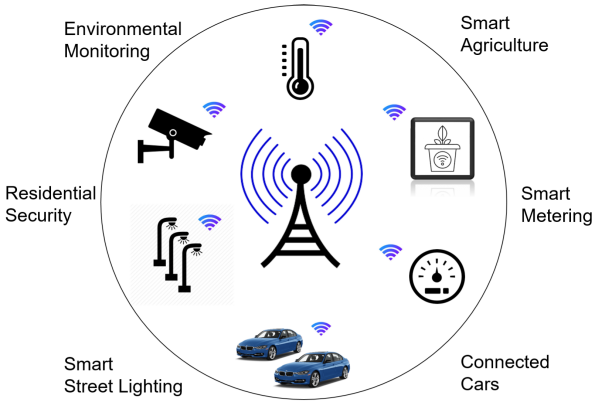

FIGURE 1. Use cases for NB-IoT.

Conception of index modulation (IM) has provided novel and different perspectives to evaluate 5G and beyond communication systems [5]. Firstly, IM has been introduced as a spatial modulation (SM) technique for multi-input multi-output (MIMO) systems by transmitting additional information bits through antenna indices [6]. IM is then applied to orthogonal frequency division multiplexing (OFDM) by activating subcarriers partially, and it is called as OFDM with index modulation (OFDM-IM) [7]. In OFDM-IM, data information is carried not only by active subcarriers but also by their indices. Combination of conventional M-ary modulation with IM in OFDM-IM provides flexible and

adaptable structure to exploit them properly regarding next-generation use cases requirements.

Fractional activation of subcarriers in OFDM-IM leads to a significant improvement on error performance under frequency selective channel, Doppler impairment and inter-carrier interference (ICI) compared with conventional OFDM [7]–[10]. Hence, it is proposed for vehicle to X (V2X) and uncoordinated networks such as massive machine-type communications (mMTC) [10], [11]. Since not all the subcarriers are activated and additional bits are carried by subcarrier indices, OFDM-IM provides power efficiency and diversity gain, too. Moreover, it allows increase on spectral efficiency for low order modulations in comparison to OFDM.

In this paper, OFDM-IM is considered as a promising candidate for NB- IoT due to motivations listed as follow.

- OFDM-IM is suitable for massive connections due to its flexible structure. Number of active subcarriers and type of M-ary modulation can be changed considering requirements of NB-IoT use case.
- OFDM-IM gives a chance to control power consumption by number of used subcarriers for data transmission.
- Limited available spectrum in NB-IoT systems results in reduced subcarrier spacing, which causes more sensitivity against ICI. Fortunately, partial subcarrier usage on OFDM-IM leads to less ICI in comparison to OFDM.
- NB-IoT is designed for low data rate up to 100 kbps [2]. Superiority of OFDM-IM against OFDM is obvious for low order modulation types. OFDM-IM provides both power efficiency and spectral efficiency for low order modulations such as binary phase shift keying (BPSK).

In order to offer low hardware complexity, direct conversion receiver (DCR) has been proposed for NB-IoT devices [12], [13]. Since DCR neither uses image rejection filters nor intermediate frequency (IF), it allows low complex receiver and low power consumption [14]. Also, it provides easier integration with massive devices in comparison to super-heterodyne receiver (SHR) due to its simple structure. However, direct conversion of a signal from baseband to radio frequency (RF) or vice versa at DCR causes more distortion at the signal. This is due to in-phase and quadrature imbalance (IQI) between modulator/demodulator branches [15], [16]. A simple receiver model with IQI is illustrated in Fig. 2. IQI corresponds to mismatches on the amplitude (ϵ) and phase ($\Delta\phi$) response of the local oscillators (LO) on I and Q branches. Ideally, both branches should consist of carriers with exactly the same signal level ($\epsilon = 0$) and $\pi/2$ phase difference ($\Delta\phi = 0$). Otherwise, IQI causes both in-band self degradation (IBSD) and in-band mirror interference (IBMI) in classical OFDM systems. In current technology OFDM, blind and data-aided iterative solutions are studied to suppress IQI impact [17]–[22]. High number of iterations in blind techniques leads to high complexity, while use of training symbols in data-aided techniques causes loss of spectral efficiency. Hence, they are not suitable for NB-IoT applications.

To the best of author's knowledge, the impact of IQI for OFDM-IM-based systems has not been studied and

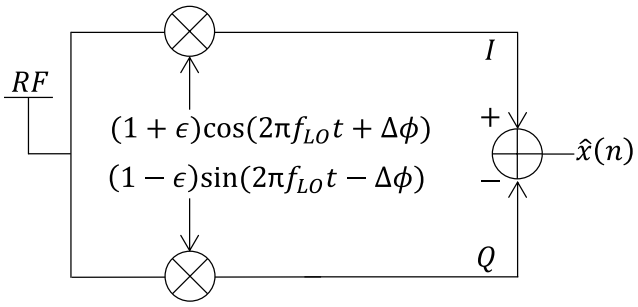

FIGURE 2. A simple direct-conversion receiver model with IQ imbalance.

characterized. In this work, frequency independent IQI is considered since IQI is independent from the frequency for narrowband communication systems [23]. This work proposes a non-iterative blind compensator to mitigate IQI by using inactive subcarriers in OFDM-IM data transmission. Compensation with OFDM-IM not only reduces low complexity but also provides less power consumption compared with iterative compensators, which are used in classical OFDM. Inactive subcarriers are used to localize IBSD and IBMI. In this way, localized IBSD and IBMI is used to estimate and compensate IQI impact. The main contributions of this paper are prioritized as follow:

- OFDM-IM is proposed for NB-IoT due to the aforementioned motivations.
- Use of DCR for NB-IoT systems causes a high IQI impact. To estimate and compensate this effect, a non-iterative receiver with OFDM-IM is proposed by exploiting inactive subcarriers during data transmission.
- Theoretical signal-to-interference-noise ratio (SINR) and average bit error probability (ABEP) analysis are performed for OFDM-IM under IQI.

The remainder of this work is organized as follows. Section 2 introduces OFDM-IM system model and IQI model. Section 3 presents proposed IQI compensator by OFDM-IM. Section 4 covers theoretical analysis for OFDM-IM considering IQI impact. Section 5 provides computer based simulation results and theoretical results. Finally, some concluding remarks are provided for NB-IoT with OFDM-IM in Section 6.

II. SYSTEM MODEL

In this section, firstly OFDM-IM system model is revised regarding a receiver with ideal RF conversion ($\epsilon = 0$, $\Delta\phi = 0$). Later, imperfect RF conversion ($\epsilon \neq 0$, $\Delta\phi \neq 0$) is considered for OFDM-IM.

A. OFDM-IM SYSTEM MODEL

In this work, it is considered a classical OFDM-IM block with N subcarriers, which are equally split into g subblocks. Block diagram of OFDM-IM transmitter is shown in Fig. 3. Each subblock contains $b = \frac{N}{g}$ subcarriers, where a out of b are selected to carry data information. Number of information

bits conveyed by indices of active subcarriers per subblock is $p_1 = \lfloor log_2 C(b, a) \rfloor$, where $C(b, a)$ and $\lfloor . \rfloor$ denote binomial coefficient and floor function, respectively. Selected subcarrier indices for l-th subblock can be expressed as

$$\xi_l = [i_l(1), \ldots, i_l(a)]_{1\times a} \tag{1}$$

where $i_l(v) \in [1, 2, \ldots, b]$. $p_2 = a(log_2 M)$ bits of information are mapped to M-ary data symbols $s_v = [s_1, \ldots, s_a]$. Transmitted symbols by selected subcarrier indices for l-th subblock is denoted as

$$X_l = [0, \ldots, s(1), 0, \ldots, s(a), \ldots, 0]_{1\times b}. \tag{2}$$

Note that if $a = b$, the system turns into a conventional OFDM system. Later, "Block Generator" entity through composition of all g subblocks generates the OFDM-IM block, which is expressed as follow

$$X = [X_1(1), \ldots, X_g(b)]_{1\times N}. \tag{3}$$

Total number of data bits assigned to one OFDM-IM block equals

$$m = gp = g(p_1 + p_2), \tag{4}$$

where $p = p_1 + p_2$ is the number of bits per OFDM-IM subblock.

Frequency domain signal X is transformed to time domain samples by Inverse Fast Fourier Transform (IFFT) after it passes through serial to parallel converter. The time domain samples of OFDM-IM symbol can be obtained as

$$x(n) = \sum_{k=0}^{N-1} X(k) e^{\frac{j2\pi nk}{N}}, \quad 0 \le n \le N-1. \tag{5}$$

A cycle prefix (CP) is generated by coping last samples of the time domain signal and appended to the beginning. CP size has to exceed maximum excess delay of the channel to prevent inter-symbol interference, which is caused by time dispersion of the channel [24]. After $x(n)$ leaves the transmitter, it undergoes through an independent and identically distributed (i.i.d.) multipath Rayleigh fading channel $h(n) = \sum_{l=0}^{L-1} h(l)\delta(n-l)$ as follow

$$y(n) = \sum_{l=0}^{L-1} h(l)x(n-l) + w(n), \tag{6}$$

where L is the number of channel taps, and path gains $h(l)$ are Gaussian random variables with $\mathcal{CN}(0, \frac{1}{L})$. $w(n)$ denotes additive white Gaussian noise (AWGN) with zero mean and variance σ_o^2.

At the receiver, CP is removed and then Fourier Transform (FFT) process is applied to the time domain signal to obtain frequency domain signal, which is expressed as

$$Y(k) = \sum_{n=0}^{N-1} y(n) e^{\frac{-j2\pi nk}{N}}, \quad 0 \le k \le N-1. \tag{7}$$

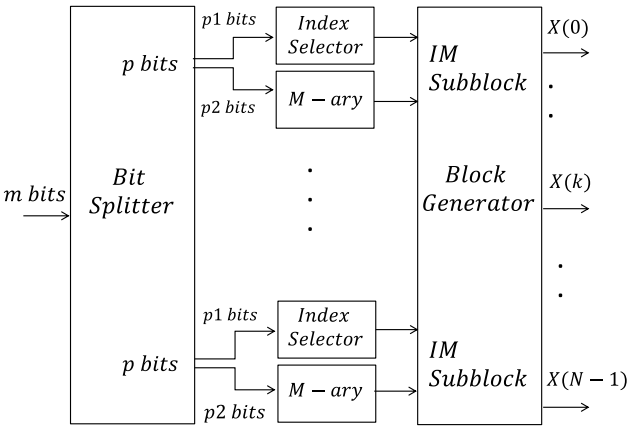

FIGURE 3. Block diagram for OFDM-IM transmitter and inverse process is performed for OFDM-IM receiver.

The frequency domain signal for the k-th subcarrier $Y(k)$ is

$$Y(k) = \underbrace{X(k)}_{\text{desired signal}} H(k) + W(k), \tag{8}$$

where $H(k)$ is channel frequency response (CFR) $\sim \mathcal{CN}(0, 1)$, and $W(k)$ represents frequency response of AWGN $\sim \mathcal{CN}(0, N_0)$.

In this work, active subcarrier indices ξ_l for l-th OFDM-IM subblock are detected by using log-likelihood ratio (LLR) receiver [25]. The receiver calculates LLR values $\lambda(k)$ for all subcarriers within the l-th subblock as

$$\lambda(k) = log\frac{a}{b-a} + \frac{|Y(k)^2|}{N_0} + log\frac{1}{M}\sum_{i=1}^{M}\frac{|Y(k) - H(k)s_i|}{N_0}. \tag{9}$$

For each subblock, a number of subcarriers with maximum λ values represent the active subcarrier indices. Then, the indices are mapped to bits to get p_1 bit stream [7]. Whilst, p_2 bit stream is obtained after demodulation of M-ary symbols, carried by the active subcarriers.

B. IQI MODEL

In a system, RF signal at the receiver $z(n)$ is converted to baseband signal $\hat{z}(n)$ via DCR. In this work, it is assumed perfect low-pass filter (LPF) and analog-to-digital converter (ADC). In general, any imperfection on gain ($\epsilon \neq 0$) and phase ($\Delta\phi \neq 0$) between sine and cosine waveforms destroys their orthogonality, as illustrated in Fig. 2. The imbalance components between I and Q branches are modeled as [22]

$$\alpha = cos(\Delta\phi) + j\epsilon sin(\Delta\phi), \tag{10}$$

$$\beta = \epsilon cos(\Delta\phi) - jsin(\Delta\phi). \tag{11}$$

The time domain baseband signal with IQI $\hat{z}(n)$ can be represented as

$$\hat{z}(n) = \alpha z(n) + \beta z^*(n), \tag{12}$$

where $(.)^*$ denotes the complex conjugate. Since FFT of complex conjugate of the time domain signal $z^*(n)$ corresponds to complex conjugate of mirror subcarrier $Z^*(-k)$, frequency domain samples of $\hat{z}(n)$ are expressed as

$$\hat{Z}(k) = \alpha Z(k) + \beta Z^*(-k), \tag{13}$$

where $-k$ represents mirror subcarrier of k-th subcarrier and vice versa. As an example, in Fig. 4, dark blue subcarrier is mirror for blue subcarrier, while blue subcarrier is mirror for dark blue subcarrier. According to (13), α represents the degradation on subcarrier k, which is named as IBSD. β represents the interference on k-th subcarrier coming from its mirror $(-k)$-th subcarrier, which is named as IBMI. If I and Q branches perfectly match, $\alpha = 1$ and $\beta = 0$. So, there is no degradation on a subcarrier, and also zero interference comes from its imaginary subcarrier.

By substituting $Y(k)$ from (8) into $Z(k)$ of (13), frequency domain signal with IQI $\hat{Y}(k)$ is expressed as

$$\hat{Y}(k) = \alpha \underbrace{X(k)}_{\text{desired signal}} H(k) + \underbrace{\beta X^*(-k)H^*(-k)}_{\text{interference}} + \underbrace{W'(k)}_{\text{amplified noise}}, \tag{14}$$

where $W'(k) = \alpha W(k) + \beta W^*(-k)$ denotes the amplification of the noise due to IQI. $W'(k) \sim \mathcal{N}(0, N_0')$ has variance as

$$N_0' = (|\alpha|^2 + |\beta|^2)N_0 = (1 + \epsilon^2)N_0, \tag{15}$$

where the amplification of noise happens only due to gain imbalance ($\epsilon \neq 0$). Since the amplified noise $\epsilon^2 N_0$ is very small can be avoided.

III. IQI MITIGATION WITH OFDM-IM

In this study, a non-iterative IQI compensator for NB-IoT systems is proposed by OFDM-IM to enhance system performance, reduce complexity and power consumption.

A visualization of (14) is illustrated in Fig. 4 for OFDM and OFDM-IM. In Fig. 4a, IQI impact is shown for OFDM where each subcarrier suffers from both IBSD and IBMI. Due to partial activation of subcarriers in OFDM-IM, not all the subcarriers are effected from both IBSD and IBMI, as shown in Fig. 4b. Moreover, IBMI does not occur on the subcarriers with null mirror, and there is no IBSD on null subcarriers. In Fig. 4b, only IBSD is present in subcarrier k_2 since there is zero interference coming from its mirror subcarrier k_1. Hence, equivalent baseband signal for active $X(k) \neq 0$ and inactive $X(-k) = 0$ is expressed as

$$D(k) = \alpha X(k)H(k) + W'(k). \tag{16}$$

Similarly, only the IBMI which is coming from mirror subcarrier k_2 is present in subcarrier k_1. In this scenario, equivalent baseband signal for inactive $X(k) = 0$ and active $X(-k) \neq 0$ is expressed as

$$I(k) = \beta X^*(-k)H^*(-k)) + W'(k). \tag{17}$$

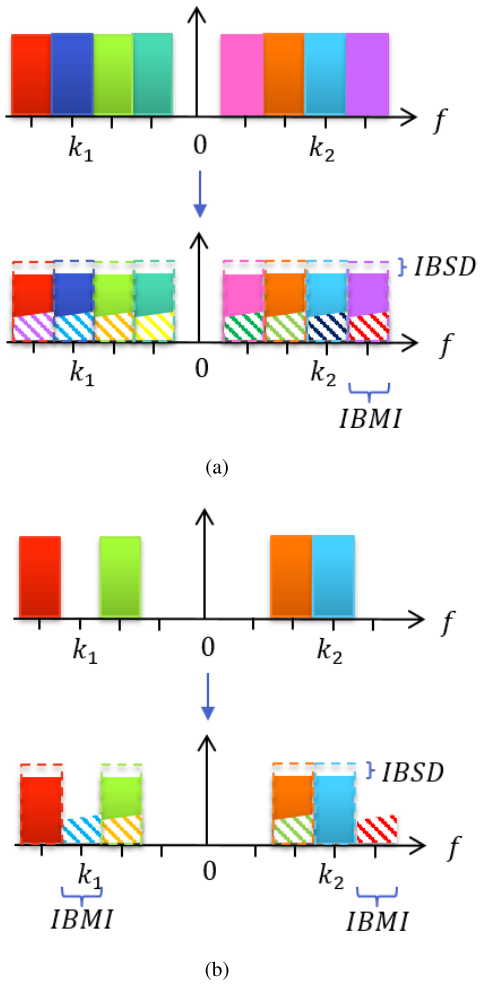

FIGURE 4. IQI impact for OFDM and OFDM-IM. (a) OFDM. (b) OFDM-IM.

Estimation of IQI parameters α and β is more complex for OFDM due to accumulation of IBSD and IBMI within a subcarrier in comparison to OFDM-IM. Therefore, an iterative estimation is required to get IQI parameters. On the other hand, there is no need to make a joined estimation for IQI components in OFDM-IM. Since $D(k)$ and $I(k)$ are linear functions of α and β regarding to (16) and (17), respectively. Therefore, α parameter is easily extracted from IBSD (16), and β is calculated from IBMI (17). In this way, α and β estimation are modeled as follow.

For active $X(k) \neq 0$ and inactive $X(-k) = 0$

$$\alpha = \frac{\hat{Y}(k)}{X(k)H(k)} + W'(k), \tag{18}$$

while for inactive $X(k) = 0$ and active $X(-k) \neq 0$

$$\beta = \frac{\hat{Y}(k)}{X^*(-k)H^*(-k)} + W'(k). \tag{19}$$

Regarding (18) and (19), subcarrier index status (active/inactive) and $X(k)$ are required to estimate the imbalance parameters α and β. To know subcarrier index status,

LLR values $\lambda(k)$ are calculated from $\hat{Y}(k)$ for each subblock at the receiver, as in (9). According to the obtained subcarrier index status, $X(k)$ is assumed as known by making a hard decision on $\hat{Y}(k)$, and is represented as $\hat{X}(k)$ [22]. Estimation of α and β components is performed by using both $\lambda(k)$ and $\hat{X}(k)$ values in one OFDM-IM block, regarding (18) and (19), respectively. To calculate ultimate α and β, all α and β values are averaged out over an OFDM-IM block. However, averaging the estimation of IQI components over more than one OFDM-IM block is needed for both high subcarrier activation ratio $\frac{a}{b}$ and IQI level. For these cases, required number of OFDM-IM blocks (N_B) is provided in Section V. The same IQI parameters, ultimate α and β, are applied to correct IQI at each block by considering (14) as

$$X'(k) = \frac{\hat{Y}(k) - \beta\hat{X}^*(-k)H^*(-k)}{\alpha H(k)}. \tag{20}$$

Later, corrected data symbols $X'(k)$ is mapped to $\hat{p}_1$ and $\hat{p}_2$ bit streams per subblock by considering the inverse process of block diagram in Fig. 3.

The main challenges for estimation of IQI components on narrowband OFDM-IM systems are active subcarrier indices detection and channel estimation. Increase on the number of active subcarriers degrades the accuracy of the proposed estimation technique. If all the subcarriers are utilized ($a = b$), OFDM-IM becomes a classical OFDM. Moreover, Cyclic Redundancy Check (CRC) algorithm is used to assess the robustness of the proposed compensator for various subcarrier activation ratio. A CRC-bit stream is appended at the end of the data bit stream per each OFDM-IM block. CRC is checked on data bits of $\hat{X}(k)$. Later, α and β components are estimated only for an OFDM-IM block with correct CRC. Necessity of CRC usage regarding activation ratio and IQI level is discussed in Section V. To assess the robustness of the proposed compensator against imperfect channel state information (CSI), intentional error Δh is added to the ideal channel $h(n)$. A complex AWGN $\sim \mathcal{N}(0, e10^{\frac{-\gamma_{idB}}{10}})$ is used to generate Δh, where e denotes the error amount of perfect CSI, and γ_{idB} represents signal-to-noise ratio (SNR) γ_i in dB scale. Therefore, imperfect CSI is expressed as $\hat{h} = h + \Delta h$ [26].

IV. THEORETICAL ANALYSIS FOR OFDM-IM UNDER IQI

This section covers theoretical analysis for OFDM-IM in the presence of IQI at the receiver. Firstly, the impact of IQI on SINR for OFDM-IM systems is evaluated and compared with conventional OFDM. Later, ABEP is calculated for OFDM-IM considering IQI. In addition, computational complexity of the proposed technique is performed.

A. SINR ANALYSIS

Regarding (14), desired signal $X(k)$ suffers from interference and amplified noise under IQI. Therefore, signal-to-interference ratio (SIR) regarding α and β parameters is expressed as

$$\gamma_I(k) = \frac{|\alpha|^2 E_s |H(k)|^2}{|\beta|^2 E_s |H^*(-k)|^2} = \frac{|\alpha|^2 \gamma_i(k)}{|\beta|^2 \gamma_i(-k)} \tag{21}$$

where $\gamma_i(k) = \frac{E_s|H(k)|^2}{N_0}$ is the SNR per subcarrier for OFDM block, and E_s is the energy per symbol. The correlation between $\gamma_i(k)$ and $\gamma_i(-k)$ is assumed to be zero since the distance between k-th subcarrier and $-k$-th subcarrier is large [27]. So, SIR can be written as

$$\gamma_I = \frac{|\alpha|^2}{|\beta|^2}. \tag{22}$$

Furthermore, the corresponding signal to interference noise ratio (SINR) is expressed as

$$\gamma(k) = \frac{|\alpha|^2 E_s |H(k)|^2}{|\beta|^2 E_s |H^*(-k)|^2 + (|\alpha|^2 + |\beta|^2)N_0}. \tag{23}$$

Therefore, $\gamma(k)$ is expressed in terms of $\gamma_I(k)$ as follow

$$\gamma(k) = \frac{1}{\frac{|\beta|^2}{|\alpha|^2} + (1 + \frac{|\beta|^2}{|\alpha|^2})\gamma_i^{-1}} = \frac{1}{\gamma_I^{-1} + (1 + \gamma_I^{-1})N_0}, \tag{24}$$

where $\gamma_I^{-1} = \frac{|\beta|^2}{|\alpha|^2}$. γ equals to γ_i if $\beta = 0$ and $\alpha = 1$, which corresponds to zero IQI scenario. In contrast with OFDM, SIR for OFDM-IM γ_{I-IM} under IQI not only depends on IQI parameters but also subcarrier activation ratio ($\frac{a}{b}$). It is shown as

$$\gamma_{I-IM} = \frac{b}{a}\frac{|\alpha|^2}{|\beta|^2}, \quad \gamma_{I-IM}^{-1} = \frac{a}{b}\frac{|\beta|^2}{|\alpha|^2}. \tag{25}$$

Hence, OFDM-IM counters with less distortion caused by IQI, which is proportional to activation ration. In this sense, (24) converts to

$$\gamma_{IM} = \frac{1}{\gamma_{I-IM}^{-1} + (1 + \gamma_{I-IM}^{-1})N_0}. \tag{26}$$

B. ABEP ANALYSIS

BER performance of OFDM-IM under IQI with maximum likelihood (ML) detector is evaluated by considering the pairwise error probability (PEP). The PEP results are valid for OFDM-IM with LLR receiver [7]. Only a single block is used to evaluate PEP, since all the subblocks are identical.

Conditional pairwise error probability (CPEP) of l-th subblock realization $\boldsymbol{X_l}$ being incorrectly detected as $\hat{\boldsymbol{X}}_l$ is given as [7]

$$P\left(\boldsymbol{X_l} \to \hat{\boldsymbol{X}}_l \,\middle|\, \boldsymbol{H_l}\right) = Q\left(\sqrt{\frac{E_s\delta}{2N_0}}\right), \tag{27}$$

where $Q(.)$ is the Gaussian Q-function. $\boldsymbol{X_l}$ and $\boldsymbol{H_l}$ are $b \times b$ all zero matrix except for their diagonal elements which represent the data symbols and the CFR for l-th subblock, respectively. δ is represented as

$$\delta = ||(\boldsymbol{X_l} - \hat{\boldsymbol{X}}_l)\boldsymbol{H_l}||^2 = \boldsymbol{H_l^H A H_l}, \tag{28}$$

where $\boldsymbol{A} = (\boldsymbol{X_l} - \hat{\boldsymbol{X}}_l)^H (\boldsymbol{X_l} - \hat{\boldsymbol{X}}_l)$, and $(.)^H$ denotes the Toeplitz Hermitian matrix. In [7], an approximation of (27) is given as

$$P\left(\boldsymbol{X_l} \to \hat{\boldsymbol{X}}_l \,\middle|\, \boldsymbol{H_l}\right) \cong \frac{e^{-\frac{E_s\delta}{4N_0}}}{12} + \frac{e^{-\frac{E_s\delta}{3N_0}}}{4}. \tag{29}$$

Therefore, the unconditional pairwise error probability (UPEP) is obtained by taking the expected value with respect to $\boldsymbol{H_l}$ as

$$P\left(\boldsymbol{X_l} \to \hat{\boldsymbol{X}}_l\right) \cong \boldsymbol{E}_{\boldsymbol{H_l}}\left\{\frac{e^{-\frac{E_s\delta}{4N_0}}}{12} + \frac{e^{-\frac{E_s\delta}{3N_0}}}{4}\right\}. \tag{30}$$

The channel correlation in frequency domain is defined as follow $\boldsymbol{C} = \boldsymbol{E}_{\boldsymbol{H_l}}\left\{\boldsymbol{H_l}\boldsymbol{H_l^H}\right\}$, which equals $\boldsymbol{Q\Gamma Q^H}$ with $\boldsymbol{\Gamma} = \boldsymbol{E}\left\{\boldsymbol{cc^H}\right\}$ and $\boldsymbol{H_l} = \boldsymbol{Qc}$. Therefore, probability density function (PDF) of $\boldsymbol{c}$ is given as

$$f(\boldsymbol{c}) = \frac{\pi^{-r}}{det(\boldsymbol{\Gamma})} e^{-\boldsymbol{c^H}\boldsymbol{\Gamma}^{-1}\boldsymbol{c}}, \tag{31}$$

where $det(.)$ represents the determinant of a matrix, and r is the rank of $\boldsymbol{C}$. After combining (30) with (31), UPEP is given as [7]

$$P\left(\boldsymbol{X_l} \to \hat{\boldsymbol{X}}_l\right) \cong \frac{1/12}{det(\boldsymbol{I} + \boldsymbol{CA}\frac{E_s}{4N_0})} + \frac{1/4}{det(\boldsymbol{I} + \boldsymbol{CA}\frac{E_s}{3N_0})}. \tag{32}$$

Regarding distortion and amplified noise in (26) due to IQI, the UPEP for OFDM-IM under IQI is expressed as

$$P\left(\boldsymbol{X_l} \to \hat{\boldsymbol{X}}_l\right) \cong \frac{1/12}{det(\boldsymbol{I} + \boldsymbol{CA}\frac{E_s}{4(\gamma_{I-IM}^{-1} + (1+\gamma_{I-IM}^{-1})N_0)})} + \frac{1/4}{det(\boldsymbol{I} + \boldsymbol{CA}\frac{E_s}{3(\gamma_{I-IM}^{-1} + (1+\gamma_{I-IM}^{-1})N_0)})}. \tag{33}$$

At last, the ABEP is calculated by considering all possible subblock realizations $v = 2^{p_1}$ of $\boldsymbol{X_l}$ and their pairwise error $\varepsilon(\boldsymbol{X_l}, \hat{\boldsymbol{X}}_l)$ as

$$P_e \cong \frac{1}{pv} \sum_{\boldsymbol{X_l}} \sum_{\hat{\boldsymbol{X}}_l} P\left(\boldsymbol{X_l} \to \hat{\boldsymbol{X}}_l\right) \varepsilon(\boldsymbol{X_l}, \hat{\boldsymbol{X}}_l). \tag{34}$$

C. COMPLEXITY ANALYSIS

From (18), complexity for α parameter estimation in terms of multiplications is

$$C_\alpha = N_B \cdot G \cdot min(a, b-a) \cdot 1C_{div}, \tag{35}$$

where C_{div} represents complex division, and it is assumed that one division equals to one multiplication. $min(a, b-a)$ denotes number of maximum used subcarriers in a subblock, which satisfy the condition $(X(k) \neq 0 \;\&\; X(-k) = 0$ or $X(k) = 0 \;\&\; X(-k) \neq 0)$ to estimate the α and β parameters, respectively. As expressed in (19), estimation of β parameter requires the same complexity with α parameter, and thus $C_\beta = C_\alpha$. According to (9), the computational complexity of the LLR detector is M multiplications per subcarrier [7]. Hence, the complexity of LLR receiver

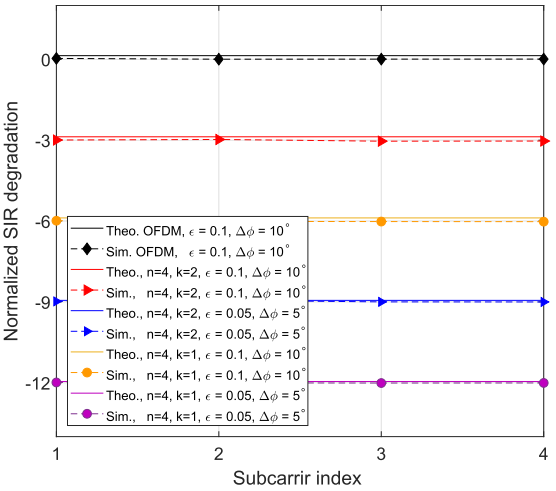

FIGURE 5. Comparison of theoretical SIR analysis and simulation results for OFDM-IM regarding to various subcarrier activation ratios and IQI parameters.

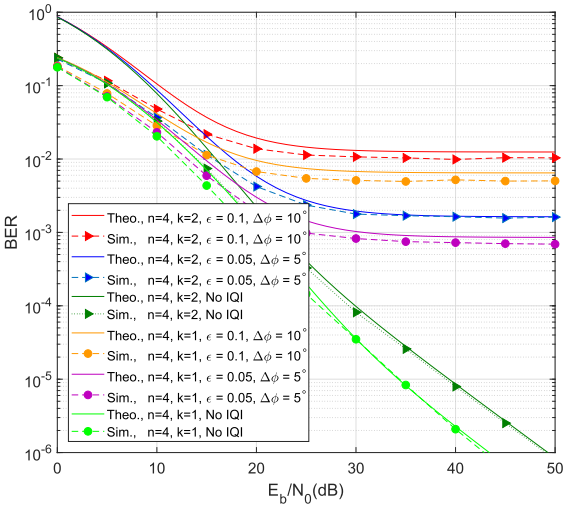

FIGURE 6. Comparison of theoretical BER analysis and simulation results for OFDM-IM regarding to various subcarrier activation ratios and IQI parameters.

for N-size OFDM-IM block is NM multiplications. Total computational complexity of the proposed technique is

$$C_{total} = N_B \cdot (NMC_{mult} + 2 \cdot G \cdot min(a, b-a) \cdot 1C_{div}), \tag{36}$$

where C_{mult} represents complex multiplication.

V. SIMULATION RESULTS AND ANALYSIS

In this section, performance of the proposed estimation and mitigation technique is evaluated for NB-IoT communication systems under IQI. Firstly, computer-based simulations are used to validate theoretical calculations for SIR and BER analysis. Later, performance of the proposed compensator is assessed by considering various subcarrier activation ratio in OFDM-IM and imperfect CSI. Moreover, computational

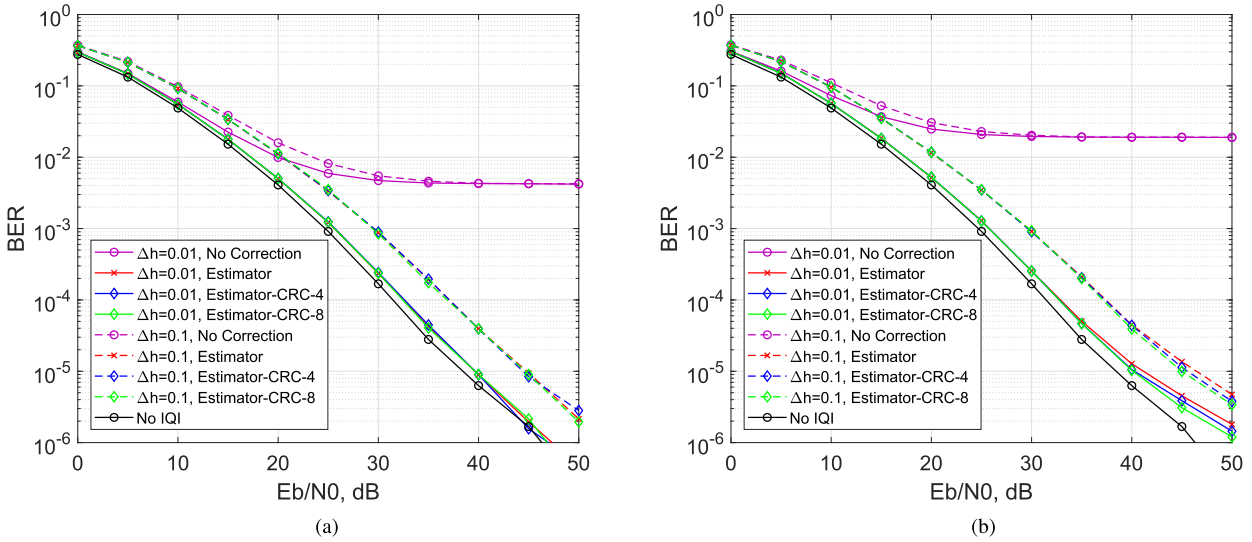

FIGURE 7. BER versus SNR performance for OFDM-IM with subblock parameters ($b = 8, a = 3$). (a) IQI parameters ($\epsilon = 0.05, \Delta\phi = 5°$). (b) IQI parameters ($\epsilon = 0.1, \Delta\phi = 10°$).

complexity of the proposed non-iterative receiver is compared with state-of-the-art blind receivers [20]. The system parameters used in the simulations are $N = 256$, $L = 10$ and $CP = 16$. IQI parameters are adjusted as ($\epsilon = 0.05$, $\Delta\phi = 5°$) and ($\epsilon = 0.1$, $\Delta\phi = 10°$), which are faced in practical scenarios [22].

Obtained results of theoretical calculations for SIR degradation caused by IQI in OFDM-IM and OFDM are illustrated in Fig. 5. It is shown that SIR calculations perfectly match with the simulation results. OFDM-IM always is exposed to less distortion than classical OFDM thanks to partial subcarrier usage. Furthermore, OFDM-IM based systems offer the advantage to control the degradation of SIR due to IQI since it is proportional with subblock activation ratio (26). In Fig. 5, for IQI parameter ($\epsilon = 0.1$, $\Delta\phi = 10°$) a 3dB more degradation is observed between lines starting from orange line ($b = 4, a = 1$) to black line ($b = 4, a = 4$) since the activation ratio increases 2 times per line. Likewise, in Fig. 6 similar behavior is observed for theoretical BER results as calculated in (33) and (34). There is a difference between theoretical and simulation BER results for low SNR since the assumed approximations become inaccurate [7], [28].

In order to show impact of different subcarrier activation ratios obviously, subblock size and number of active subcarriers are choosen as $b = 8$ and $a = 3, 5$, respectively. Spectral efficiency of OFDM-IM for ($b = 8, a = 3$) and ($b = 8, a = 5$) are the same with conventional OFDM, and equals to $\frac{m}{N+L} = 0.941$bits/s/Hz.

For all simulations in Fig. 7 and Fig. 8, active subcarriers carry BPSK modulated data symbols. "No IQI" refers to results without IQI, and "No Correction" refers to results without the proposed compensator under IQI. "Estimator" refers to results with the compensator. In addition, estimator is combined with CRC algorithm to assess accuracy of decision on the selected subcarrier index status. "CRC-V" denotes V-number of CRC bits added to the end of OFDM-IM block. Moreover, two levels of imperfect CSI are used in the simulations as well as perfect CSI ($\Delta h = 0$). $\Delta h = 0.01$ refers to low error on CSI, while $\Delta h = 0.10$ represent high error on CSI. It is important to mention that in both Fig. 7 and Fig. 8, solid lines and dashed lines represent the results for $\Delta h = 0.01$ and $\Delta h = 0.1$, respectively.

In Fig. 7, OFDM-IM with ($b = 8, a = 3$) is simulated. Proposed non-iterative compensator by OFDM-IM perfectly mitigates low level IQI ($\epsilon = 0.05$, $\Delta\phi = 5°$), as shown in Fig. 7(a). Performance of the proposed compensator does not change with imperfect CSI, which causes shift for all the results regarding to level of imperfection (Δh). Subcarrier index status (active/inactive) is correctly detected since low activation ratio ($\frac{a}{b} = \frac{3}{8}$) leads to low SIR degradation caused by IQI. Hence, use of CRC bits does not further improve the BER performance for the proposed technique, as seen in the Fig. 7(a). Increase of the IQI parameters ($\epsilon = 0.1$, $\Delta\phi = 10°$) for the same activation ratio poses more degradation on BER performance, as illustrated in Fig. 7(b). The proposed compensator mitigates the impact of high IQI thanks to low activation ratio. Therefore, use of CRC algorithm is not required for low subcarrier activation ratios.

Although the same IQI parameters are used in Fig. 7 and Fig. 8, BER performance becomes worse in Fig. 8 due to increase on the number of active subcarriers ($b = 8, a = 5$). An activation ratio ($\frac{5}{8}$) increases the probability of facing both IBSD and IBII for a given subcarrier. Therefore, finding the right subcarrier index status becomes a challenge. In Fig. 8(a), the compensator provides similar results with Fig. 7(b) due to lower IQI parameters, even for higher activation ratio. In Fig. 8(b), the compensator has the worst performance since IQI level increases to ($\epsilon = 0.1$, $\Delta\phi = 10°$) as well as

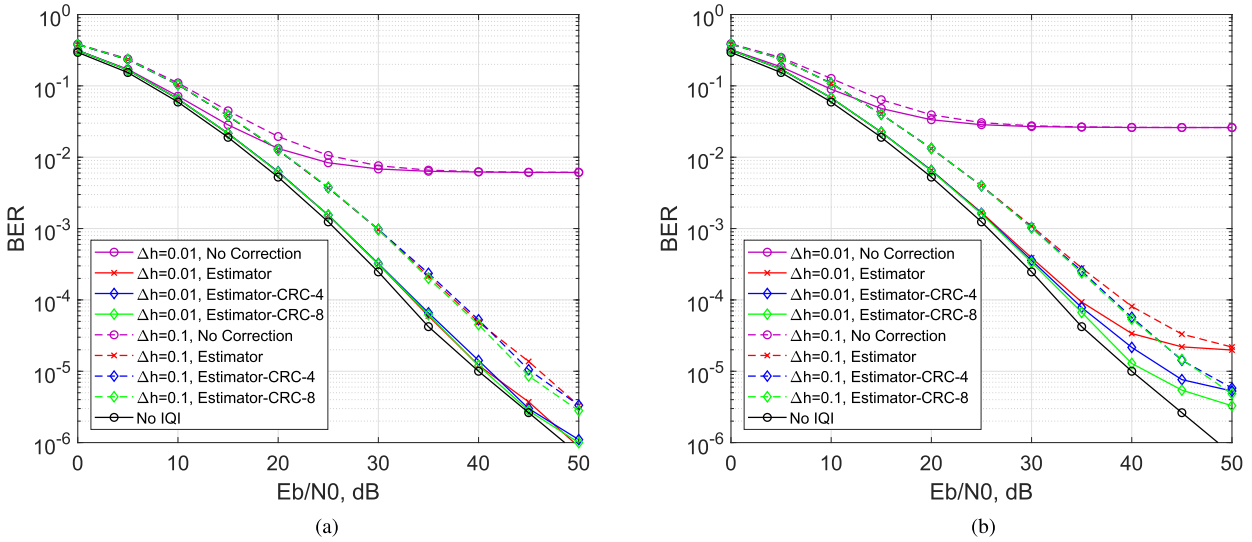

FIGURE 8. BER versus SNR performance for OFDM-IM with subblock parameters ($b = 8, a = 5$). (a) IQI parameters ($\epsilon = 0.05, \Delta\phi = 5°$). (b) IQI parameters ($\epsilon = 0.1, \Delta\phi = 10°$).

high activation ratio. Hence, reliability of estimated subcarrier index status decreases. Use of CRC bits to select utilized subcarriers increases the reliability, thus improvement is observed on BER. In addition, 8-bit CRC does not provide a considerable improvement on the BER with respect to 4-bit CRC. Hence, short CRC bit streams can be used for high subcarrier activation ratio and IQI level.

State-of-the-art blind estimators by utilizing least-mean-squares (LMS) and recursive-least-squares (RLS) are compared with the proposed technique, since the estimators are proposed for frequency independent IQI [20]. It is observed that two algorithms need around 1500 iterations to estimate IQI components. Estimation by LMS and RLS algorithms need $5C_{mult}$ and $9C_{mult}$ per iteration, respectively. The computational complexity of the proposed method for the used system parameters ($a = 3, b = 8, \epsilon = 0.05, \Delta\phi = 5°, N_B = 1$) is $704C_{mult}$, according to (36). Estimation of IQI components is performed through one OFDM-IM block. However, averaging the estimation of IQI components over more than one block is needed for both high subcarrier activation ratio and IQI level ($a = 5, b = 8, \epsilon = 0.1, \Delta\phi = 10°, N_B = 5$). The results show that no more than 5 OFDM-IM blocks are required to estimate the IQI parameters, with computational complexity of $3520C_{mult}$.

In all figures, it is observed a significant degradation on the error performance when the IQI distorts the signal. The proposed non-iterative technique considerably mitigates the effect of IQI for OFDM-IM in NB-IoT communication systems.

VI. CONCLUSION

NB-IoT devices require low hardware complexity, low cost and low power consumption for deployment flexibility. Use of DCR, which is recommended for NB-IoT, results in sensitivity against IQI. Hence, there is a need for solutions to mitigate IQI impact. In this paper, a practical receiver for IQI estimation and compensation is proposed, studied and evaluated both using computer simulations and theoretical analysis. Outcome of this work shows that proposed receiver mitigates IQI for NB-IoT. It is seen that almost perfectly mitigation for IQI faced in real scenarios. Therefore, we expect that our technique will be useful for NB-IoT applications. Unlike suppression techniques that are used in classical OFDM, where iterative approach is needed, a non-iterative approach is introduced. There is a critical difference between OFDM-IM and OFDM, which enables to use non-iterative approach on proposed receiver. In this specific study, we focus on NB-IoT, and therefore frequency independent IQI is studied. Further studies will investigate frequency-dependent IQI for wideband IoT systems.

REFERENCES

[1] Ericsson, "Cellular networks for massive IoT," White Paper Uen 284 23-3278, Jan. 2016.
[2] *Cellular System Support for Ultra Low Complexity and Low Throughput Internet of Things*, document TR 45.820 V13.1.0, 3GPP, Nov. 2015.
[3] Y.-P. E. Wang *et al.*, "A primer on 3GPP narrowband Internet of Things," *IEEE Commun. Mag.*, vol. 55, no. 3, pp. 117–123, Mar. 2017.
[4] A. Al-Fuqaha, M. Guizani, M. Mohammadi, M. Aledhari, and M. Ayyash, "Internet of Things: A survey on enabling technologies, protocols, and applications," *IEEE Commun. Surveys Tuts.*, vol. 17, no. 4, pp. 2347–2376, 4th Quart., 2015.
[5] E. Başar, M. Wen, R. Mesleh, M. Di Renzo, Y. Xiao, and H. Haas, "Index modulation techniques for next-generation wireless networks," *IEEE Access*, vol. 5, pp. 16693–16746, May 2017.
[6] R. Y. Mesleh, H. Haas, S. Sinanovic, C. W. Ahn, and S. Yun, "Spatial modulation," *IEEE Trans. Veh. Technol.*, vol. 57, no. 4, pp. 2228–2241, Jul. 2008.
[7] E. Başar, Ü. Aygölü, E. Panayırcı, and H. V. Poor, "Orthogonal frequency division multiplexing with index modulation," *IEEE Trans. Signal Process.*, vol. 61, no. 22, pp. 5536–5549, Nov. 2013.
[8] G. D. Ntouni, V. M. Kapinas, and G. K. Karagiannidis, "On the optimal tone spacing for interference mitigation in OFDM-IM systems," *IEEE Commun. Lett.*, vol. 21, no. 5, pp. 1019–1022, May 2017.

[9] Q. Ma, P. Yang, Y. Xiao, H. Bai, and S. Li, "Error probability analysis of OFDM-IM with carrier frequency offset," *IEEE Commun. Lett.*, vol. 20, no. 12, pp. 2434–2437, Dec. 2016.
[10] X. Cheng, M. Wen, L. Yang, and Y. Li, "Index modulated OFDM with interleaved grouping for V2X communications," in *Proc. IEEE 17th Int. Conf. Intell. Transp. Syst. (ITSC)*, Oct. 2014, pp. 1–8.
[11] S. Doğan, A. Tusha, and H. Arslan, "OFDM with index modulation for asynchronous mMTC networks," *Sensors*, vol. 18, no. 4, p. 1280, Apr. 2018.
[12] A. Burdett, "Ultra-low-power wireless systems: Energy-efficient radios for the Internet of Things," *IEEE Solid-State Circuits Mag.*, vol. 7, no. 3, pp. 18–28, Mar. 2015.
[13] I.-G. Lee, "Digital pre-distortion of carrier frequency offset for reliable Wi-Fi enabled IoTs," *Future Internet*, vol. 9, no. 3, p. 46, Mar. 2017.
[14] A. A. Abidi, "Direct-conversion radio transceivers for digital communications," *IEEE J. Solid-State Circuits*, vol. 30, no. 12, pp. 1399–1410, Dec. 1995.
[15] B. Razavi, *RF Microelectronics*. Upper Saddle River, NJ, USA: Prentice-Hall, 1998.
[16] A. ElSamadouny, A. Gomaa, and N. Al-Dhahir, "Likelihood-based spectrum sensing of OFDM signals in the presence of Tx/Rx I/Q imbalance," in *Proc. IEEE Global Commun. Conf. (GLOBECOM)*, Dec. 2012, pp. 1–6.
[17] C.-L. Liu, "Impacts of I/Q imbalance on QPSK-OFDM-QAM detection," *IEEE Trans. Consum. Electron.*, vol. 44, no. 3, pp. 984–989, Aug. 1998.
[18] H. Arslan, "IQ gain imbalance measurement for OFDM based wireless communication systems," in *Proc. IEEE Mil. Commun. Conf. (MILCOM)*, Oct. 2006, pp. 1–5.
[19] H. A. Mahmoud, H. Arslan, M. K. Ozdemir, and F. E. Retnasothie, "IQ imbalance correction for OFDMA uplink systems," in *Proc. IEEE Int. Conf. Commun. (ICC)*, Jun. 2009, pp. 1–5.
[20] W. Nam, H. Roh, J. Lee, and I. Kang, "Blind adaptive I/Q imbalance compensation algorithms for direct-conversion receivers," *IEEE Signal Process. Lett.*, vol. 19, no. 8, pp. 475–478, Aug. 2012.
[21] M. Valkama, M. Renfors, and V. Koivunen, "Advanced methods for I/Q imbalance compensation in communication receivers," *IEEE Trans. Signal Process.*, vol. 49, no. 10, pp. 2335–2344, Oct. 2001.
[22] J. Tubbax, B. Come, L. Van der Perre, L. Deneire, S. Donnay, and M. Engels, "Compensation of IQ imbalance in OFDM systems," in *Proc. IEEE Int. Conf. Commun. (ICC)*, May 2003, pp. 1–9.
[23] Y. Li, *In-Phase and Quadrature Imbalance*. New York, NY, USA: Springer, 2014.
[24] J. B. Andersen, T. S. Rappaport, and S. Yoshida, "Propagation measurements and models for wireless communications channels," *IEEE Commun. Mag.*, vol. 33, no. 1, pp. 42–49, Jan. 1995.
[25] M. Wen, Y. Zhang, J. Li, E. Başar, and F. Chen, "Equiprobable subcarrier activation method for OFDM with index modulation," *IEEE Commun. Lett.*, vol. 20, no. 12, pp. 2386–2389, Dec. 2016.
[26] J. M. Hamamreh and H. Arslan, "Secure orthogonal transform division multiplexing (OTDM) waveform for 5G and beyond," *IEEE Commun. Lett.*, vol. 21, no. 5, pp. 1191–1194, May 2017.
[27] Ö. Özdemir, R. Hamila, and N. Al-Dhahir, "Exact average OFDM subcarrier SINR analysis under joint transmit–receive I/Q imbalance," *IEEE Trans. Veh. Technol.*, vol. 63, no. 8, pp. 4125–4130, Oct. 2014.
[28] T. Mao, Z. Wang, Q. Wang, S. Chen, and L. Hanzo, "Dual-mode index modulation aided OFDM," *IEEE Access*, vol. 5, pp. 50–60, 2017.

ARMED TUSHA received the B.Sc. degree in electrical and electronics engineering from Istanbul Sehir University, Istanbul, Turkey, in 2016. He is currently pursuing the M.Sc. degree with the Communications, Signal Processing, and Networking Center, Istanbul Medipol University, Istanbul. His current research interests include digital communications, signal processing techniques, multicarrier schemes, orthogonal/non-orthogonal multiple accessing in wireless networks, index modulation, and channel coding.

SEDA DOĞAN received the B.Sc. degree in electronics and telecommunication engineering from Kocaeli University, Kocaeli, Turkey, in 2015. She is currently pursuing the Ph.D. degree with the Communications, Signal Processing, and Networking Center, Istanbul Medipol University, Istanbul, Turkey. Her current research interests include millimeter-wave frequency bands, index modulation, synchronous/asynchronous communication, and random access techniques for next-generation applications.

HÜSEYİN ARSLAN (S'95–M'98–SM'04–F'15) received the B.S. degree from Middle East Technical University, Ankara, Turkey, in 1992, and the M.S. and Ph.D. degrees from Southern Methodist University, Dallas, TX, USA, in 1994 and 1998, respectively. From 1998 to 2002, he was with the Research Group, Ericsson Inc., Charlotte, NC, USA, where he was involved in several projects related to 2G and 3G wireless communication systems. Since 2002, he has been with the Electrical Engineering Department, University of South Florida, Tampa, FL, USA. Since 2014, he has also been the Dean of the College of Engineering and Natural Sciences, Istanbul Medipol University. He was a part-time Consultant for various companies and institutions, including Anritsu Company, Morgan Hill, CA, USA, and the Scientific and Technological Research Council of Turkey. His research interests are in physical layer security, millimeter-wave communications, small cells, multicarrier wireless technologies, coexistence issues on heterogeneous networks, aeronautical (high-altitude platform) communications, *in vivo* channel modeling, and system design.